We are IntechOpen, the world's leading publisher of Open Access books Built by scientists, for scientists

4,800
Open access books available

122,000
International authors and editors

135M
Downloads

Our authors are among the

154
Countries delivered to

TOP 1%
most cited scientists

12.2%
Contributors from top 500 universities

CLARIVATE ANALYTICS BOOK CITATION INDEX INDEXED

WEB OF SCIENCE™

Selection of our books indexed in the Book Citation Index in Web of Science™ Core Collection (BKCI)

Interested in publishing with us?
Contact book.department@intechopen.com

Numbers displayed above are based on latest data collected.
For more information visit www.intechopen.com

18

New Approach to Ultra-Fast All-Optical Signal Processing Based on Quantum Dot Devices

Y. Ben Ezra, B.I. Lembrikov
Holon Institute of Technology (HIT),P.O.Box 305, 58102, 52 Golomb Str., Holon Israel

1. Introduction

Fiber-optic technology is characterized by enormous potential capabilities: huge bandwidth up to nearly $50Tb/s$ due to a high frequency of an optical carrier, low signal attenuation of about $0.2dB/km$, low signal distortion, low power requirement, low material usage, small space requirement, and low cost Agrawal (2002), Mukherjee (2001).
However, the realization of these capabilities requires very high-bandwidth transport network facilities which cannot be provided by existing networks consisting of electronic components of the transmitters and receivers, electronic switches and routers Agrawal (2002). Most current networks employ electronic signal processing and use optical fiber as a transmission medium. Switching and signal processing are realized by an optical signal down-conversion to an electronic signal, and the speed of electronics cannot match the optical fiber bandwidth Ramamurthy (2001). For instance, a single-mode fiber (SMF) bandwidth is nearly $50Tb/s$, which is nearly four orders of magnitude higher than electronic data rates of a few Gb/s Mukherjee (2001). Typically, the maximum rate at which a gateway that interfaces with lower-speed subnetworks can access the network is limited by an electronic component speed up to a few tens of Gb/s. These limitations may be overcome by the replacement of electronic components with ultra-fast all-optical signal processing components such as fiber gratings, fiber couplers, fiber interferometers Agrawal (2001), semiconductor optical amplifiers (SOAs) Dong (2008), Hamié (2002), SOA and quantum dot SOA (QD-SOA) based monolithic Mach-Zehnder interferometers (MZIs) Joergensen (1996), Wang (2004), Sun (2005), Kanellos (2007), Wada (2007), Ben-Ezra (2008), Ben-Ezra (2009), all-optical switches based on multilayer system with enhanced nonlinearity and carbon nanotubes Wada (2007).
SOAs are among the most promising candidates for all-optical processing devices due to their high-speed capability up to $160Gb/s$, low switching energy, compactness, and optical integration compatibility Dong (2008). Their performance may be substantially improved by using QD-SOAs characterized by a low threshold current density, high saturation power, broad gain bandwidth, and a weak temperature dependence as compared to bulk and multi-quantum well (MQW) devices Bimberg (1999), Sugawara (2004), Ustinov (2003).
High-speed wavelength conversion, logic gate operations, and signal regeneration are important operations of the all-optical signal processing where SOAs are widely used Agrawal (2002), Ramamurthy (2001), Dong (2008).
A wavelength converter (WC) changes the input wavelength to a new wavelength without modifying the data content of a signal Agrawal (2002). Wavelength conversion is essential for optical wavelength division multiplexing (WDM) network operation Ramamurthy (2001).

There exist several all-optical techniques for wavelength conversion based on SOAs using the cross gain modulation (XGM) and cross phase modulation (XPM) effects between the pulsed signal and the continuous wave (CW) beam at the wavelength at which the converted signal is desired Agrawal (2002). In particular, MZI with a SOA inserted in each arm is characterized by a high on-off contrast and the output converted signal consisting of the exact replica of the incident signal Agrawal (2002).
All-optical logic operations are important for all-optical signal processing Sun (2005). All-optical logic gates operation is based on nonlinearities of optical fibers and SOAs. However, the disadvantages of optical fibers are weak nonlinearity, long interaction length, and/or high control energy required in order to achieve a reasonable switching efficiency Sun (2005). On the contrary, SOAs, and especially QD-SOAs, possess high nonlinearity, small dimensions, low energy consumption, high operation speed, and can be easily integrated into photonic and electronic systems Sun (2005), Hamié (2002), Kanellos (2007), Dong (2008).
The major problems of the improving transmission optical systems emerge from the signal-to-noise ratio (SNR) degradation, chromatic dispersion, and other impairment mechanisms Zhu (2007). For this reason, the optical signal reamplification, reshaping, and retiming (3R), or the so-called 3R regeneration, is necessary in order to avoid the accumulation of noise, crosstalk and nonlinear distortions and to provide a good signal quality for transmission over any path in all-optical networks Sartorius (2001), Zhu (2007), Leem (2006), Kanellos (2007). Optical regeneration technology can work with lower power, much more compact size, and can provide transparency in the needed region of spectrum Zhu (2007). All-optical 3R regeneration should be also less complex, and use fewer optoelectronics/electronics components than electrical regeneration providing better performance Leem (2006). All-optical 3R regenerator for different length packets at $40Gb/s$ based on SOA-MZI has been recently demonstrated Kanellos (2007).
We developed for the first time a theoretical model of an ultra-fast all-optical signal processor based on the QD SOA-MZI where XOR operation, WC, and 3R signal regeneration can be simultaneously carried out by AO-XOR logic gates for bit rate up to $(100-200)\,Gb/s$ depending on the value of the bias current $I \sim (30-50)\,mA$ Ben-Ezra (2009). We investigated theoretically different regimes of RZ optical signal operation for such a processor and carried out numerical simulations. We developed a realistic model of QD-SOA taking into account two energy levels in the conduction band of each QD and a Gaussian distribution for the description of the different QD size Ben-Ezra (2007), Ben-Ezra (2009), unlike the one-level model of the identical QDs recently used Berg (2004a), Sun (2005). We have shown that the accurate description of the QD-SOA dynamics predicts the high quality output signals of the QD SOA-MZI based logic gate without significant amplitude distortions up to a bit rate of about $100Gb/s$ for the bias current $I = 30mA$ and $200Gb/s$ for the bias current $I = 50mA$ being limited by the relaxation time of the electron transitions between the wetting layer (WL), the excited state (ES) and the ground state (GS) in a QD conduction band Ben-Ezra (2009).
The chapter is constructed as follows. The QD structure, electronic and optical properties are discussed in Section 2. The dynamics of QD SOA, XGM and XPM phenomena in QD SOA are described in Section 3. The theory of ultra-fast all-optical processor based on MZI with QD SOA is developed in Section 4. The simulation results are discussed in Section 5. Conclusions are presented in Section 6.

2. Structure, Electronic and Optical Properties of Quantum Dots (QDs)

Quantization of electron states in all three dimensions results in a creation of a novel physical object - a macroatom, or quantum dot (QD) containing a zero dimensional electron gas. Size

quantization is effective when the quantum dot three dimensions are of the order of magnitude of the electron de Broglie wavelength which is about several nanometers Ustinov (2003). An electron-hole pair created by light in a QD has discrete energy eigenvalues caused by the electron-hole confinement in the material. As a result, QD has unique electronic and optical properties that do not exist in bulk semiconductor material Ohtsu (2008).
QDs based on different technologies and operating in different parts of spectrum are known such as In(Ga)As QDs grown on GaAs substrates, InAs QDs grown on InP substrates, and colloidal free-standing InAs QDs. QD structures are commonly realized by a self-organized epitaxial growth where QDs are statistically distributed in size and area. A widely used QDs fabrication method is a direct synthesis of semiconductor nanostructures based on the island formation during strained-layer heteroepitaxy called the Stranski-Krastanow (SK) growth mode Ustinov (2003). The spontaneously growing QDs are said to be self-assembling. The energy shift of the emitted light is determined by size of QDs that can be adjusted within a certain range by changing the amount of deposited QD material. Smaller QDs emit photons of shorter wavelengths Ustinov (2003). The main advantages of the SK growth are following Ustinov (2003).

1. SK growth permits the preparation of extremely small QDs in a maskless process without lithography and etching which makes it a promising technique to realize QD lasers.
2. A great number of QDs is formed in one simple deposition step.
3. The synthesized QDs have a high uniformity in size and composition.
4. QDs can be covered epitaxially by host material without any crystal or interface defects.

The simplest QD models are a spherical QD with a radius R, and a parallelepiped QD with a side length $L_{x,y,z}$. The spherical QD is described by the spherical boundary conditions for an electron or a hole confinement which results in the electron and hole energy spectra $E_{e,nlm}$ and $E_{h,nlm}$ given by, respectively Ohtsu (2008)

$$E_{e,nlm} = E_g + \frac{\hbar^2}{2m_e}\left(\frac{\alpha_{nl}}{R}\right)^2; E_{h,nlm} = \frac{\hbar^2}{2m_h}\left(\frac{\alpha_{nl}}{R}\right)^2 \tag{1}$$

where

$$n = 1, 2, 3, ...; l = 0, 1, 2, ...n-1; m = 0, \pm 1, \pm 2, .. \pm l \tag{2}$$

E_g is the QD semiconductor material band gap, $m_{e,h}$ are the electron and hole effective mass, respectively, $\hbar = h/2\pi$, h is the Planck constant, and α_{nl} is the n-th root of the spherical Bessel function. The parallelepiped QD is described by the boundary conditions at its corresponding surfaces, which yield the energy eigenvalues $E_{e,nlm}$ and $E_{h,nlm}$ given by, respectively Ohtsu (2008)

$$E_{e,nlm} = E_g + \frac{\hbar^2\pi^2}{2m_e}\left[\left(\frac{n}{L_x}\right)^2 + \left(\frac{l}{L_y}\right)^2 + \left(\frac{m}{L_z}\right)^2\right] \tag{3}$$

$$E_{h,nlm} = \frac{\hbar^2\pi^2}{2m_h}\left[\left(\frac{n}{L_x}\right)^2 + \left(\frac{l}{L_y}\right)^2 + \left(\frac{m}{L_z}\right)^2\right], n, l, m = 1, 2, 3, ... \tag{4}$$

The density of states $\rho_{QD}(E)$ for an array of QDs has the form Ustinov (2003)

$$\rho_{QD}(E) = \sum_n \sum_m \sum_l 2n_{QD}\delta\left(E - E_{e,nlm}\right) \tag{5}$$

where $\delta\left(E - E_{e,nlm}\right)$ is the δ-function, and n_{QD} is the surface density of QDs.
The optical spectrum of QDs consists of a series of transitions between the zero-dimensional electron gas energy states where the selections rules are determined by the form and symmetry of QDs Ustinov (2003). The finite carrier lifetime results in Lorentzian broadening of a finite width Ustinov (2003).
Detailed theoretical and experimental investigations of InAs/GaAs and InAs QDs electronic structure taking into account their more realistic lens or pyramidal shape, size, composition profile, and production technique have been carried out Bimberg (1999), Bányai (2005), Ustinov (2003). A system of QDs can be approximated with a three energy level model in the conduction band containing a spin degenerate ground state GS, fourfold degenerate excited state (ES) with comparatively large energy separations of about $50 - 70meV$, and a narrow continuum wetting layer (WL). The electron WL is situated $150meV$ above the lowest electron energy level in the conduction band, i.e. GS and has a width of approximately $120meV$. In real cases, the QDs vary in size, shape, and local strain which leads to the fluctuations in the quantized energy levels and the inhomogeneous broadening in the optical transition energy. A Gaussian distribution may be used for the description of the QD sizes, and it shows that the discrete resonances merge into a continuous structure with widths around 10% Bányai (2005). The QDs and WL are surrounded by a barrier material which prevents direct coupling between QD layers. The absolute number of states in the WL is much larger than in the QDs. GS and ES in QDs are characterized by homogeneous and inhomogeneous broadening Bányai (2005). The homogeneous broadening caused by the scattering of the optically generated electrons and holes with imperfections, impurities, phonons, or through the radiative electron-hole pair recombination Bányai (2005) is about $15meV$ at room temperature Sugawara (2002). The inhomogeneous broadening in the optical transition energy is due to the QDs variations in size, shape, and local strain Bányai (2005), Sugawara (2004), Ustinov (2003).
In(Ga)As/GaAs QDs are characterized by emission at wavelengths no longer than $\lambda = 1.35\mu m$, while the InAs/InP QDs have been proposed for emission at the usual telecommunication wavelength $\lambda = 1.55\mu m$ Ustinov (2003).

3. Structure and Operation Mode of QD SOA

In this section, we will discuss the theory of QD SOA operation based on the electron rate equations and photon propagation equation Qasaimeh (2003), Qasaimeh (2004), Ben-Ezra (2005a), Ben-Ezra (2005b), Ben-Ezra (2007).

3.1 Basic Equations of QD SOA Dynamics

The active region of a QD SOA is a layer including self-assembled InGaAs QDs on a GaAs substrate Sugawara (2004). Typically, the QD density per unit area is about $\left(10^{10} - 10^{11}\right) cm^{-2}$. The bias current is injected into the active layer including QDs, and the input optical signals are amplified via the stimulated emission or processed via the optical nonlinearity by QDs Sugawara (2004). The stimulated radiative transitions occur between GS and the valence band of QDs. A detailed theory of QD SOAs based on the density matrix approach has been developed in the pioneering work Sugawara (2004) where the linear and nonlinear optical responses of QD SOAs with arbitrary spectral and spatial distribution of quantum dots in active region under the multimode light propagation have been considered. It has been shown theoretically that XGM takes place due to the coherent terms under the condition that the mode separation is comparable to or less than the polarization relaxation rate $|\omega_m - \omega_n| \leq \Gamma_g$ where $\omega_{m,n}$ are the mode frequencies and the relaxation time $\tau = \Gamma_g^{-1} = 130fs$ Sugawara

(2004). XGM is also possible in the case of the incoherent nonlinear polarization, or the so-called incoherent spectral hole burning Sugawara (2004). XGM occurs only for signals with a detuning limited by the comparatively small homogeneous broadening, and for this reason the ensemble of QDs should be divided into groups by their resonant frequency of the GS transition between the conduction and valence bands Sugawara (2004).
The phenomenological approach to the QD SOA dynamics is based on the rate equations for the electron densities of GS, ES and for combined WL and barrier serving as a reservoir. It is determined by electrons, because of the much larger effective mass of holes and their smaller state spacing Berg (2004a). Recently, an attempt has been carried out to take into account the hole dynamics for small-signal XGM case Kim (2009).
In the QD SOA-MZI, optical signals propagate in an active medium with the gain determined by the rate equations for the electron transitions in QD-SOA between WL, GS and ES Qasaimeh (2003), Qasaimeh (2004), Ben-Ezra (2005a), Ben-Ezra (2008). Unlike the model with the one energy level in the conduction band Berg (2004a), Sun (2005), we have taken into account the two energy levels in the conduction band: GS and ES Ben-Ezra (2007), Ben-Ezra (2009). The diagram of the energy levels and electron transitions in the QD conduction band is shown in Fig. 1.

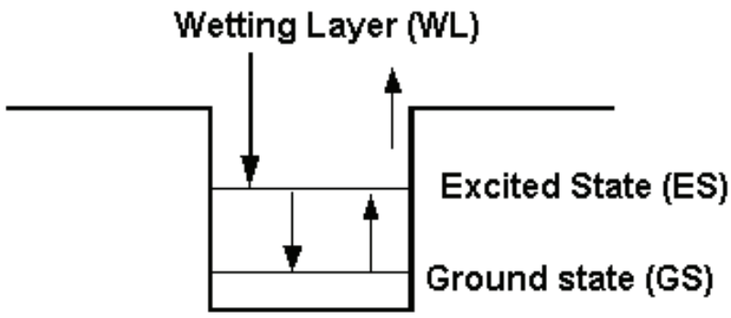

Fig. 1. Energy levels and electron transitions in a QD conduction band

The stimulated and spontaneous radiative transitions occur from GS to the QD valence band level. The system of the rate equations accounts for the following transitions:

1. the fast electron transitions from WL to ES with the relaxation time $\tau_{w2} \sim 3ps$;
2. the fast electron transitions between ES and GS with the relaxation time from ES to GS $\tau_{21} = 0.16ps$ and the relaxation time from GS to ES $\tau_{12} \sim 1.2ps$;
3. the slow electron escape transitions from ES back to WL with the electron escape time $\tau_{2w} \sim 1ns$.

The balance between the WL and ES is determined by the shorter time τ_{w2} of QDs filling. Carriers relax quickly from the ES level to the GS level, while the former serves as a carrier reservoir for the latter Berg (2001). In general case, the radiative relaxation times depend on the bias current. However, it can be shown that for moderate values of the WL carrier density $N_w \sim \left(10^{14} - 10^{15}\right) cm^{-3}$ this dependence can be neglected Berg (2001), Berg (2004b). The spontaneous radiative time in QDs $\tau_{1R} \gtrsim (0.4 - 0.5)\, ns$ remains large enough Sakamoto (2000), Qasaimeh (2003), Qasaimeh (2004), Sugawara (2004), Matthews (2005).
The carrier dynamics is characterized by slow relaxation processes between WL and ES. The rapidly varying coherent nonlinear population terms vanish after the averaging over the comparatively large relaxation time τ_{w2} ∼several ps from the two-dimensional WL to the ES. We

have taken into account only incoherent population terms because for XGM between modes with the maximum detuning $\Delta\lambda_{\max} = 30nm$ within the especially important in optical communications conventional band of $\lambda = (1530 \div 1565)\, nm$ the condition $\omega_1 - \omega_2 > \Gamma_g^{-1}$ is valid even for the lowest relaxation time from the ES to GS $\tau_{21} = 0.16ps$, and the rapidly varying coherent beating terms are insignificant Sugawara (2004). The direct carrier capture into the GS is neglected due to the fast intradot carrier relaxation and the large energy separation between the GS and the WL and it is assumed that the charge neutrality condition in the GS is valid. The rate equations have the form Qasaimeh (2003), Qasaimeh (2004), Ben-Ezra (2007).

$$\frac{\partial N_w}{\partial t} = \frac{J}{eL_w} - \frac{N_w\,(1-h)}{\tau_{w2}} + \frac{N_w h}{\tau_{2w}} - \frac{N_w}{\tau_{wR}}, \tag{6}$$

$$\frac{\partial h}{\partial t} = \frac{N_w L_w\,(1-h)}{N_Q \tau_{w2}} - \frac{N_w L_w h}{N_Q \tau_{2w}} - \frac{(1-f)\,h}{\tau_{21}} + \frac{f\,(1-h)}{\tau_{12}}, \tag{7}$$

$$\frac{\partial f}{\partial t} = \frac{(1-f)\,h}{\tau_{21}} - \frac{f\,(1-h)}{\tau_{12}} - \frac{f^2}{\tau_{1R}} - \frac{g_p L}{N_Q}\,(2f-1)\,S_p \frac{c}{\sqrt{\varepsilon_r}} - \frac{g_s L}{N_Q}\,(2f-1)\,S_s \frac{c}{\sqrt{\varepsilon_r}}. \tag{8}$$

Here, S_p, S_s are the CW pump and on-off-keying (OOK) modulated signal wave photon densities, respectively, L is the length of SOA, g_p, g_s are the pump and signal wave modal gains, respectively, f is the electron occupation probability of GS, h is the electron occupation probability of ES, e is the electron charge, t is the time, τ_{wR} is the spontaneous radiative lifetime in WL, N_Q is the surface density of QDs, L_w is the effective thickness of the active layer, ε_r is the SOA material permittivity, c is the velocity of light in free space.The modal gain $g_{p,s}(\omega)$ is given by Uskov (2004)

$$g_{p,s}(\omega) = \frac{2\Gamma N_Q}{a} \int d\omega F(\omega)\,\sigma(\omega_0)\,(2f-1) \tag{9}$$

where the number l of QD layers is assumed to be $l = 1$, the confinement factor Γ is assumed to be the same for both the signal and the pump waves, a is the mean size of QDs, $\sigma(\omega_0)$ is the cross section of interaction of photons of frequency ω_0 with carriers in QD at the transition frequency ω including the homogeneous broadening factor, $F(\omega)$ is the distribution of the transition frequency in the QD ensemble which is assumed to be Gaussian Qasaimeh (2004), Uskov (2004). It is related to the inhomogeneous broadening and it is described by the expression Uskov (2004)

$$F(\omega) = \frac{1}{\Delta\omega\sqrt{\pi}} \exp\left[-\frac{(\omega-\overline{\omega})^2}{(\Delta\omega)^2}\right] \tag{10}$$

where the parameter $\Delta\omega$ is related to the inhomogeneous linewidth $\gamma_{in\,\mathrm{hom}} = 2\sqrt{\ln 2}\Delta\omega$, and $\overline{\omega}$ is the average transition frequency.

3.2 XGM and XPM in QD SOA

XGM and XPM in QD SOA are determined by the interaction of QDs with optical signals. The optical signal propagation in a QD SOA is described by the following truncated equations for the slowly varying CW and pulse signals photon densities $S_{CW,P} =$

$P_{CW,P}/\left(\hbar\omega_{CW,P}\left(v_g\right)_{CW,P}A_{eff}\right)$ and phases $\theta_{CW,P}$ Agrawal (1989).

$$\frac{\partial S_{CW,P}\left(z,\tau\right)}{\partial z}=\left(g_{CW,P}-\alpha_{int}\right)S_{CW,P}\left(z,\tau\right) \tag{11}$$

$$\frac{\partial\theta_{CW,P}}{\partial z}=-\frac{\alpha}{2}g_{CW,P} \tag{12}$$

Here $P_{CW,P}$ are the CW and pulse signal optical powers, respectively, A_{eff} is the QD SOA effective cross-section, $\omega_{CW,P}$, $\left(v_g\right)_{CW,P}$ are the CW and pulse signal group angular frequencies and velocities, respectively, $g_{CW,P}$ are the active medium (SOA) gains at the corresponding optical frequencies, α_{int} is the absorption coefficient of the SOA material, α is a linewidth enhancement factor (LEF) which describes the coupling between gain and refractive index changes in the material and determines the frequency chirping Agrawal (2002). For the pulse propagation analysis, we replace the variables (z,t) with the retarded frame variables $\left(z,\tau=t\mp z/v_g\right)$. For optical pulses with a duration $T\gtrsim 10ps$ the optical radiation of the pulse is filling the entire active region of a QD SOA of the length $L\lesssim 1mm$ and the propagation effects can be neglected Gehrig (2002). Hence, in our case the photon densities

$$S_{CW,P}\left(z,\tau\right)=\left(S_{CW,P}\left(\tau\right)\right)_{in}\exp\left[\int_0^z\left(g_{CW,P}-\alpha_{int}\right)dz'\right] \tag{13}$$

can be averaged over the QD SOA length L which yields

$$S_{CW,P}\left(\tau\right)=\frac{1}{L}\left(S_{CW,P}\left(\tau\right)\right)_{in}\int_0^L dz\exp\left[\int_0^z\left(g_{CW,P}-\alpha_{int}\right)dz'\right] \tag{14}$$

Solution of equation (12) yields for the phases

$$\theta_{CW,P}\left(\tau\right)=-\left(\alpha/2\right)\int_0^L dz g_{CW,P}. \tag{15}$$

The time-dependent variations of the carrier distributions in the QDs and WL result in the strong phase changes (12) during the light propagation in the QD SOA Gehrig (2002). System of equations (6)-(8) with the average pump and signal photon densities (14) and phases (15) constitutes a complete set of equations describing XGM and XPM in QD SOA related by the LEF α as it is seen from equations (11), (12) and (15).

In order to investigate the possibility of XGM in QD SOAs due to the connections between different QDs through WL at detunings between a signal and a pumping larger than the homogeneous broadening we modified equations (6)-(8) dividing QDs into groups similarly to Sugawara (2002), Sugawara (2004), Sakamoto (2000). We consider a limiting case of the groups 1 and 2 with a detuning substantially larger than the homogeneous broadening, in order to investigate the possibility that they are related only due to the carrier relaxation from WL to ES Ben-Ezra (2007). The rate equations for such QDs take the form

$$\frac{\partial N_w}{\partial t}=\frac{J}{eL_w}-\frac{N_w\left(1-h_1\right)}{\tau_{w2}}+\frac{N_w h_1}{\tau_{2w}}-\frac{N_w}{\tau_{wR}}$$

$$- \frac{N_w\left(1-h_2\right)}{\tau_{w2}} + \frac{N_w h_2}{\tau_{2w}}, \tag{16}$$

$$\frac{\partial h_{1,2}}{\partial t} = \frac{N_w L_w\left(1-h_{1,2}\right)}{N_Q \tau_{w2}} - \frac{N_w L_w h_{1,2}}{N_Q \tau_{2w}} - \frac{\left(1-f_{1,2}\right) h_{1,2}}{\tau_{21}} + \frac{f_{1,2}\left(1-h_{1,2}\right)}{\tau_{12}}, \tag{17}$$

$$\frac{\partial f_{1,2}}{\partial t} = \frac{\left(1-f_{1,2}\right) h_{1,2}}{\tau_{21}} - \frac{f_{1,2}\left(1-h_{1,2}\right)}{\tau_{12}} - \frac{f_{1,2}^2}{\tau_{1R}} - \frac{g_{p,s} L}{N_Q}\left(2f_{1,2}-1\right) S_{p,s} \frac{c}{\sqrt{\varepsilon_r}} \tag{18}$$

where the indices 1,2 correspond to the groups 1 and 2 of QDs. Equations (17)-(18) contain the electron occupation probabilities belonging to the same group and the photon density corresponding to the optical beam resonant with respect to this group, while the WL rate equation (16) includes the contributions of the both groups.

4. Theory of an Ultra-Fast All-Optical Processor

4.1 Theoretical Approach

The theoretical analysis of the proposed ultra-fast QD SOA-MZI processor is based on the combination of the MZI model with the nonlinear characteristics and the QD-SOA dynamics. The block diagram of the processor is shown in Fig. 2.

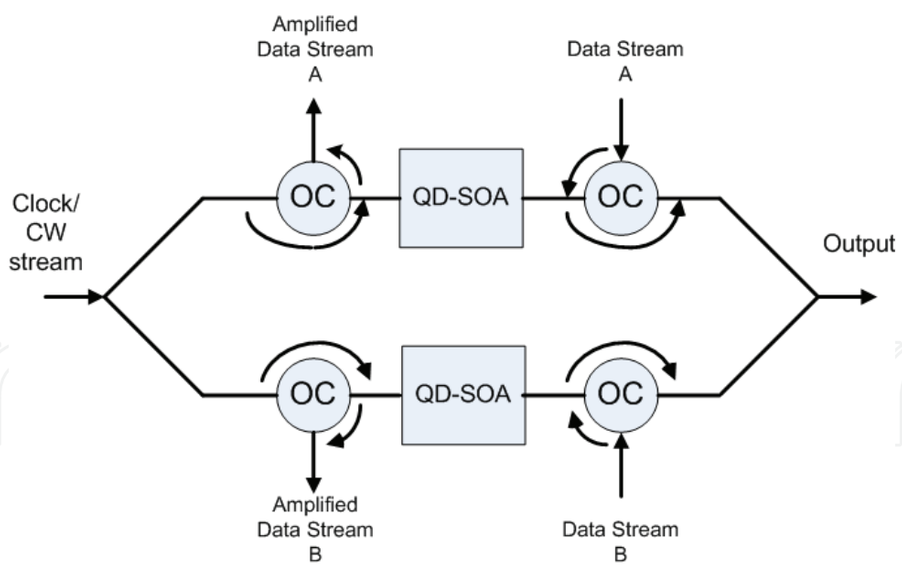

Fig. 2. A block diagram of the ultra-fast MZI processor containing in each arm a QD SOA, 50-50 3dB optical couplers, and optical circulators (OC)

At the output of MZI, the CW optical signals from the two QD SOAs interfere giving the output intensity Sun (2005), Wang (2004).

$$P_{XOR} = \frac{P_{in}}{4}\left\{G_1\left(t\right) + G_2\left(t\right)\right.$$

$$-2\sqrt{G_1(t)\,G_2(t)}\cos\left[\phi_1(t)-\phi_2(t)\right]\} \tag{19}$$

where P_{in} is the CW or the clock stream optical signal divided and introduced via the symmetric coupler into the two QD-SOAs, $G_{1,2}(t)=\exp(g_{1,2}L_{1,2})$, $g_{1,2}$, $L_{1,2}$, and $\phi_{1,2}(t)$ are the time-dependent gain, the SOA gain, the active medium length, and phase shift, respectively, in the two arms of QD SOA-MZI. The phases $\phi_{1,2}(t)$ should be inserted into equation (19) from equation (15). When the control signals A and/or B are fed into the two SOAs they modulate the gain of the SOAs and give rise to the phase modulation of the co-propagating CW signal due to LEF α Agrawal (2001), Agrawal (2002), Newell (1999). LEF values may vary in a large interval from the experimentally measured value of LEF $\alpha=0.1$ in InAs QD lasers near the gain saturation regime Newell (1999) up to the giant values of LEF $\alpha=60$ recently measured in InAs/InGaAs QD lasers Dagens (2005). However, such limiting cases can be achieved for specific electronic band structure Newell (1999), Dagens (2005), Sun (2004). The typical values of LEF in QD lasers are $\alpha\approx(2-7)$ Sun (2005). Detailed measurements of the LEF dependence on injection current, photon energy, and temperature in QD SOAs have also been carried out Schneider (2004). For low-injection currents, the LEF of the dot GS transition is between 0.4 and 1 increasing up to about 10 with the increase of the carrier density at room temperature Schneider (2004). The phase shift at the QD SOA-MZI output is given by Wang (2004)

$$\phi_1(t)-\phi_2(t)=-\frac{\alpha}{2}\ln\left(\frac{G_1(t)}{G_2(t)}\right) \tag{20}$$

It is seen from equation (20) that the phase shift $\phi_1(t)-\phi_2(t)$ is determined by both LEF and the gain. For the typical values of LEF $\alpha\approx(2-7)$, gain $g_{1,2}=11.5cm^{-1}$, $L_{1,2}=1500\mu m$ the phase shift of about π is feasible.

4.2 Logic Gate Operation

Consider an AO-XOR gate based on integrated QD SOA-MZI which consists of a symmetrical MZI where one QD SOA is located in each arm of the interferometer as shown in Fig. 2. Two optical control beams A and B at the same wavelength λ are inserted into ports A and B of MZI separately. A third signal, which represents a clock stream of continuous series of unit pulses is split into two equal parts and injected into the two SOAs. The detuning $\Delta\omega$ between the signals A, B and the third signal should be less than the homogeneous broadening of QDs spectrum. In such a case the ultrafast operation occurs. In the opposite case of a sufficiently large detuning comparable with the inhomogeneous broadening, XGM in a QD SOA is also possible due to the interaction of QDs groups with essentially different resonance frequencies through WL for optical pulse bit rates up to $10Gb/s$ Ben-Ezra (2007). When $A=B=0$, the signal at the MZI input port traveling through the two arms of the SOA acquires a phase difference of π when it recombines at the output port, and the output is "0" due to the destructive interference. When $A=1$, $B=0$, the signal traveling through the arm with signal A acquires a phase change due to XPM between the pulse train A and the signal. The signal traveling through the lower arm does not have this additional phase change which results in an output "1" Sun (2005). The same result occurs when $A=0$, $B=1$ Sun (2005). When $A=1$ and $B=1$ the phase changes for the signal traveling through both arms are equal, and the output is "0".

4.3 Wavelength Conversion

An ideal wavelength convertor (WC) should have the following properties: transparency to bit rates and signal formats, fast setup time of output wavelength, conversion to both shorter

and longer wavelengths, moderate input power levels, possibility for no conversion regime, insensitivity to input signal polarization, low-chirp output signal with high extinction ratio and large SNR, and simple implementation Ramamurthy (2001). Most of these requirements can met by using SOA in the process of wavelength conversion. XGM method using SOAs is especially attractive due to its simple realization scheme for WC Agrawal (2001). However, the main disadvantages of this method are substantial phase distortions due to the frequency chirping, degradation due to spontaneous emission, and a relatively low extinction ratio Agrawal (2001). These parameters may be improved by using QD-SOAs instead of bulk SOAs due to pattern-effect-free high-speed wavelength conversion of optical signals by XGM, a low threshold current density, a high material gain, high saturation power, broad gain bandwidth, and a weak temperature dependence as compared to bulk and MQW devices Ustinov (2003). We combine the advantages of QD-SOAs as a nonlinear component and MZI as a system whose output signal can be easily controlled. In the situation where one of the propagating signals A or B is absent, CW signal with the desired output wavelength is split asymmetrically to each arm of MZI and interferes at the output either constructively or destructively with the intensity modulated input signal at another wavelength. The state of interference depends on the relative phase difference between the two MZI arms which is determined by the SOAs. In such a case the QD SOA-MZI operates as an amplifier of the remaining propagating signal. Then, the operation with the output "1" may be characterized as a kind of WC due to XGM between the input signal A or B and the clock stream signal. The possibility of the pattern-effect-free wavelength conversion by XGM in QD SOAs has been demonstrated experimentally at the wavelength of $1.3\mu m$ Sugawara (2004).

4.4 3R Regeneration

Short optical pulses propagating in optical fibers are distorted due to the fiber losses caused by material absorption, Rayleigh scattering, fiber bending, and due to the broadening caused by the material, waveguide, polarization-mode, and intermodal dispersion Agrawal (2001), Agrawal (2002). 3R regeneration is essential for the successful logic operations because of the ultra-fast data signal distortions. 3R regeneration requires an optical clock and a suitable architecture of the regenerator in order to perform a clocked decision function Sartorius (2001). In such a case, the shape of the regenerated pulses is defined by the shape of the clock pulses Sartorius (2001).

The proposed QD SOA-MZI ultra-fast all-optical processor can successfully solve three problems of 3R regeneration. Indeed, the efficient pattern–effect free optical signal re-amplification may be carried out in each arm by QD-SOAs. WC based on the all-optical logic gate provides the re-shaping since noise cannot close the gate, and only the data signals have enough power to close the gate Sartorius (2001). The re-timing in QD-SOA-MZI based processor is provided by the optical clock which is also essential for the re-shaping Sartorius (2001). Hence, if the CW signal is replaced with the clock stream, the 3R regeneration can be carried out simultaneously with logic operations. The analysis shows that for the strongly distorted data signals a separate processor is needed providing 3R regeneration before the data signal input to the logic gate.

5. Simulation Results and Discussion

The study of the ultrafast all-optical signal processor in different regimes such as XOR, WC, 3R signal regeneration requires the simultaneous analysis of the QD-SOA dynamics and MZI behavior. The MZI performance efficiency is determined by the combination of XGM and

XPM processes, and for this reason it strongly depends on the value of LEF which varies in an interval of $\alpha \sim (0.1 - 7)$ Newell (1999), Sun (2005). For small $\alpha < 1$ the XPM process is too weak, and the MZI efficiency is very low. However, the analysis shows that for $\alpha \geq 1$ and for the bias current values of $I = 30mA$ the system efficiency is large enough. The efficiency may be significantly increased by using larger values of the bias current for the same value of LEF α.

System of equations (6)-(8) with the average pump and signal photon densities (14) constituting a complete set of equations describing XGM and XPM in QD SOA are essentially nonlinear and extremely complicated. Their analytical solution in a closed form is hardly possible, and for this reason, the system of equations (6)-(8) has been solved numerically for the following typical values of the QD-SOA based AO-XOR Berg (2001), Uskov (2004), Qasaimeh (2003), Qasaimeh (2004): $L = 1500\mu m$, $L_w = 0.1\mu m$, the bias current $I = 30mA$, LEF $\alpha = 1$, the width of QD-SOA $W = 10\mu m$, $\Gamma \sim 3 \times 10^{-2}$, $\tau_{w2} = 3ps$; $\tau_{21} = 0.16ps$; $\tau_{12} = 1.2ps$; $\tau_{1R} = 0.4ns$; $\tau_{2w} = \tau_{wR} = 1ns$, $N_Q = 5 \times 10^{10} cm^{-2}$, $\alpha_{int} = 3cm^{-1}$, $\sigma_E = 30meV$, $\tau_{12} = \tau_{21}\rho \exp(\Delta E_{21}/k_B T)$. Here $\rho = 1$, $\Delta E_{21} = 50meV$ is the separation between the ES and GS energy levels, k_B is the Boltzmann constant, $T = 300K$ is the temperature. The situation when only one data signal interacts with the clock stream signal is shown in Fig. 3.

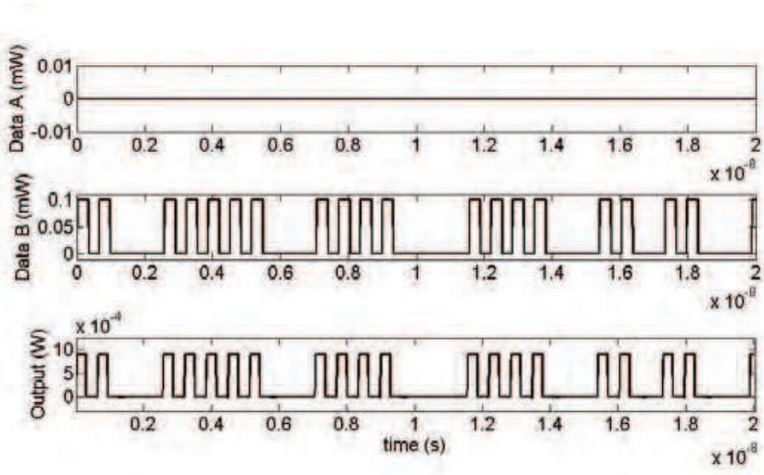

Fig. 3. Wavelength conversion realization by XGM between the data signal B with $\lambda_B = 1560nm$ and the clock stream signal with $\lambda_p = 1530nm$ for the signal bit rate $2.5Gb/s$

In such a case, wavelength conversion occurs between the optical signal B at the wavelength $\lambda_B = 1560nm$ propagating through the lower arm of QD SOA-MZI and the clock stream signal with $\lambda_p = 1530nm$. Pattern-effect free wavelength conversion can be realized for the bit rate up to $100Gb/s$ in the case of a detuning less than the homogeneous broadening, and up to $10Gb/s$ for a large detuning comparable to the inhomogeneous broadening Ben-Ezra (2007).

Input optical signal distortions result in the output signal pattern-effect, significant pulse broadening and overlapping accompanied by information losses. In such a case the form of pulses can be essentially improved by using the 3R regeneration process shown in Fig. 4 where the RZ clock stream is fed into the input port instead of a CW signal.

It is seen in Fig. 4 that a distorted pulse duration is almost doubled while the regenerated signals shown with a solid line have a regular structure with the equal amplitudes and a shape defined by the clock.

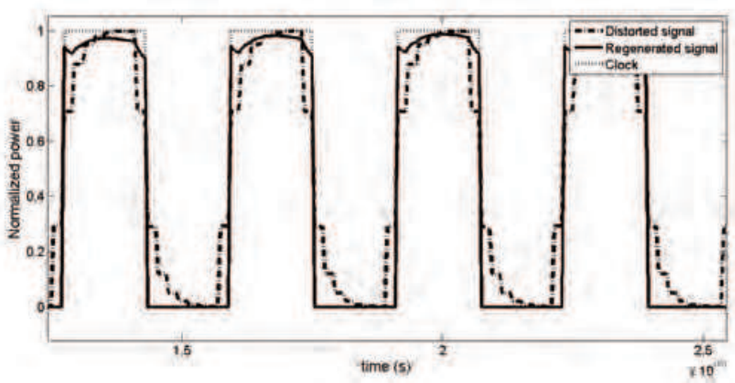

Fig. 4. Optical signal 3R regeneration process

The simultaneous XOR logic operation, wavelength conversion and 3R regeneration for the distorted at the input RZ signals A and B with the wavelengths $\lambda_A = 1550nm$ and $\lambda_B = 1560nm$ for the bit rate of 100Gb/s are shown in Fig. 5. Here the RZ clock stream is fed into the input port instead of a CW signal in order to carry out 3R regeneration.

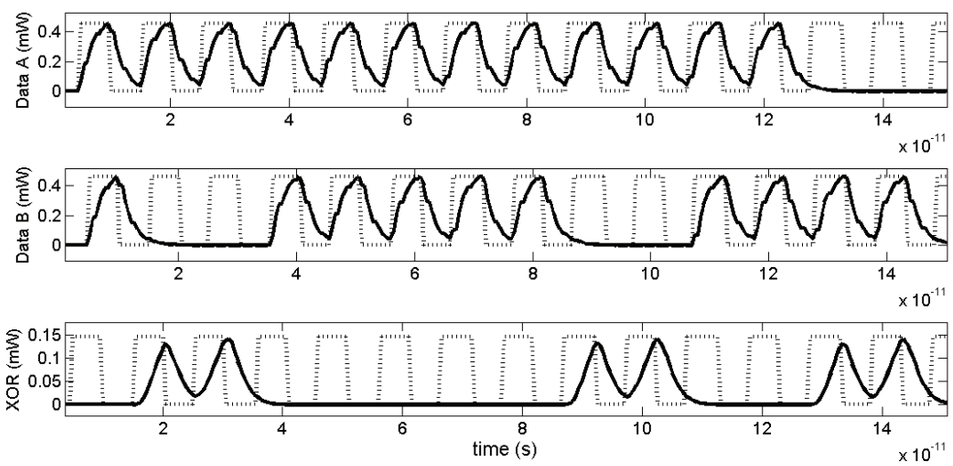

Fig. 5. Simultaneous logic XOR operation, wavelength conversion and 3R regeneration of the distorted RZ signals A, B with $\lambda_A = 1550nm$, $\lambda_B = 1560nm$, and the clock stream (dashed line) at the input port. The bit rate is $100Gb/s$.

The ultrafast all-optical signal processor operation performance is mainly determined by the electron dynamics in QD-SOA. In order to investigate the QD-SOA behavior in both arms of QD SOA-MZI we have solved numerically system of equations (6)-(8). The temporal dependence of the electron concentration in WL $N_w(t)$ and the electron occupation probability of GS and ES, $f(t)$ and $h(t)$, respectively, in the QD-SOA situated in the upper arm of the MZI for the signal repetition rates of $50Gb/s$, $100Gb/s$, and $250Gb/s$ are presented in Figs. 6, 7, 8, respectively.

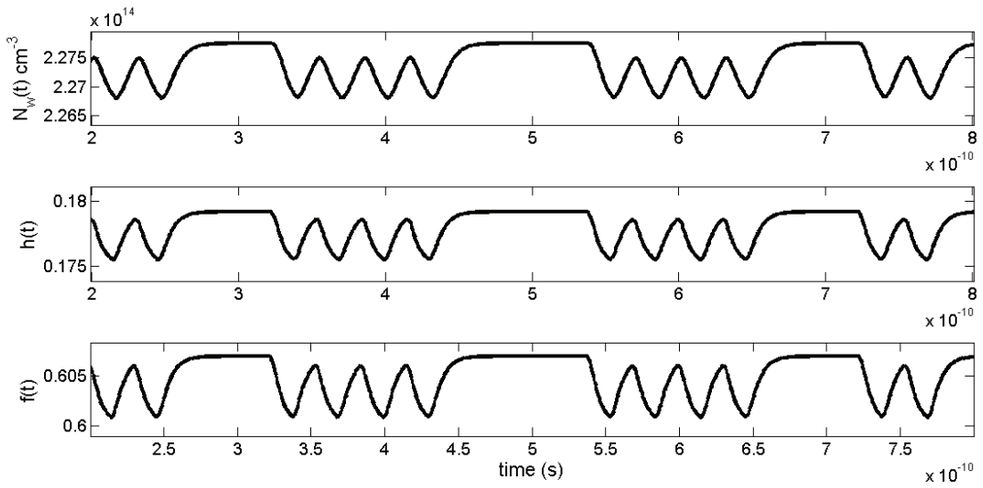

Fig. 6. emporal dependence of the electron concentration in WL $N_w\,(t)$, the electron occupation probability of GS $f\,(t)$, and the electron occupation probability of ES $h\,(t)$ for the QD SOA in the upper arm of the QD SOA-MZI with a clock stream at a data signal repetition rate of $50Gb/s$

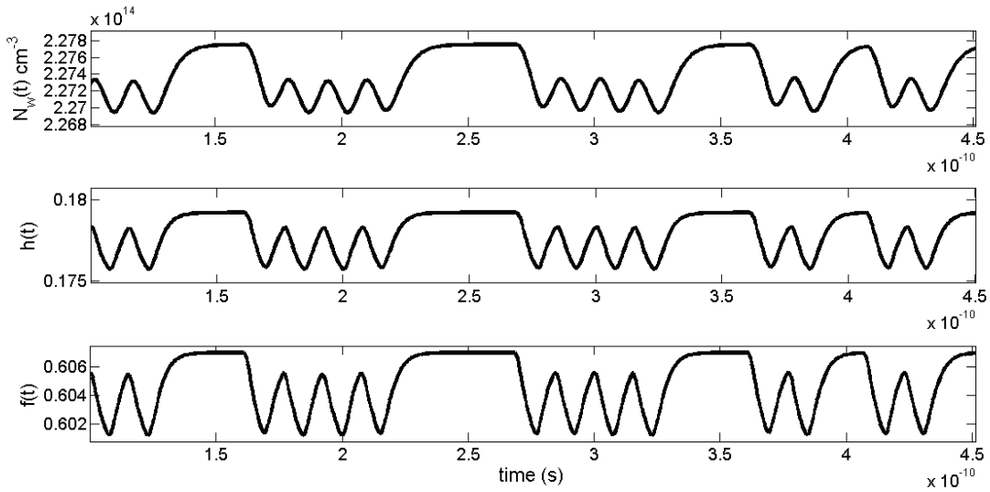

Fig. 7. emporal dependence of the electron concentration in WL $N_w\,(t)$, the electron occupation probability of GS $f\,(t)$, and the electron occupation probability of ES $h\,(t)$ for the QD SOA in the upper arm of the QD SOA-MZI with a clock stream at a data signal repetition rate of $100Gb/s$

The analysis of QD SOA dynamics for the signal detuning smaller than the homogeneous broadening clearly shows that the operation rate of QD-SOAs is limited by the relaxation time $\tau_{w2} \sim (3-5)\,ps$ for the electron transitions between WL and ES in the resonant QDs. At the bit rate of several dozens of Gb/s the oscillations of both WL and ES strictly follow the input optical signal variation.

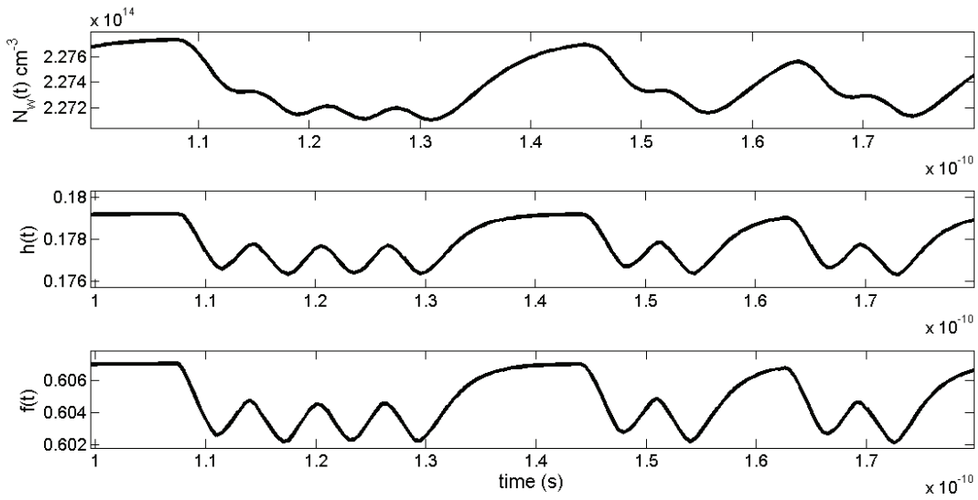

Fig. 8. emporal dependence of the electron concentration in WL $N_w\left(t\right)$, the electron occupation probability of GS $f\left(t\right)$, and the electron occupation probability of ES $h\left(t\right)$ for the QD SOA in the upper arm of the QD SOA-MZI with a clock stream at a data signal repetition rate of $250Gb/s$

The electron population of GS is supported at a comparatively high level $f \gtrsim 0.6$ due to the electron fast transitions between ES and GS. The ES population is low because ES level is emptied rapidly by the fast stimulated transitions to GS at the comparatively high input optical power $P_{in} \gtrsim 5mW$. The operation rate of QD-SOA can be increased due to the acceleration of the gain recovery at the high optical signal power and the large bias currents $I \sim 30mA$ Ben-Ezra (2008), Ben-Ezra (2005b). The filling of ES is determined by slower transitions from WL with the relaxation time $\tau_{w2} \sim (3-5)\, ps$. It is seen from the temporal dependences of $N_w\left(t\right)$, $h\left(t\right)$ and $f\left(t\right)$ in the lower arm QD-SOA for the pulse bit rate of $50Gb/s$, $100Gb/s$, and $250Gb/s$ shown in Figs. 6, 7, 8, respectively, that the WL electron population gradually fails to follow the rapid changes of the input optical signals. At $250Gb/s$ the oscillation form of the GS and ES occupation probabilities also deteriorates.
Consequently, the gain in the both arms of QD SOA-MZI as well as the input power P_{XOR} (19) and phase difference (20) cannot be controlled anymore. Indeed, as it is seen from Figs. 9, 10 for the operation rate of about $250Gb/s << \tau_{w2}^{-1}$ the performance of AO-XOR gate sharply deteriorates due to retardation of the QD-SOA dynamics. The increase of the bias current improves the system performance. However, typically the bias current values for QD-SOAs are of an order of magnitude of $50mA$, which corresponds to the current density of several hundred A/cm^2 Ustinov (2003).

6. Conclusions

We for the first time developed a theoretical model of a QD SOA-MZI based ultra-fast all-optical signal processor which under certain conditions can simultaneously carry out logic gates XOR operation, wavelength conversion, and 3R regeneration of the moderately distorted optical signals. The QD SOA-MZI operation has been analyzed theoretically by solving the rate equations of the QD-SOA dynamics, optical wave propagation equations in an active

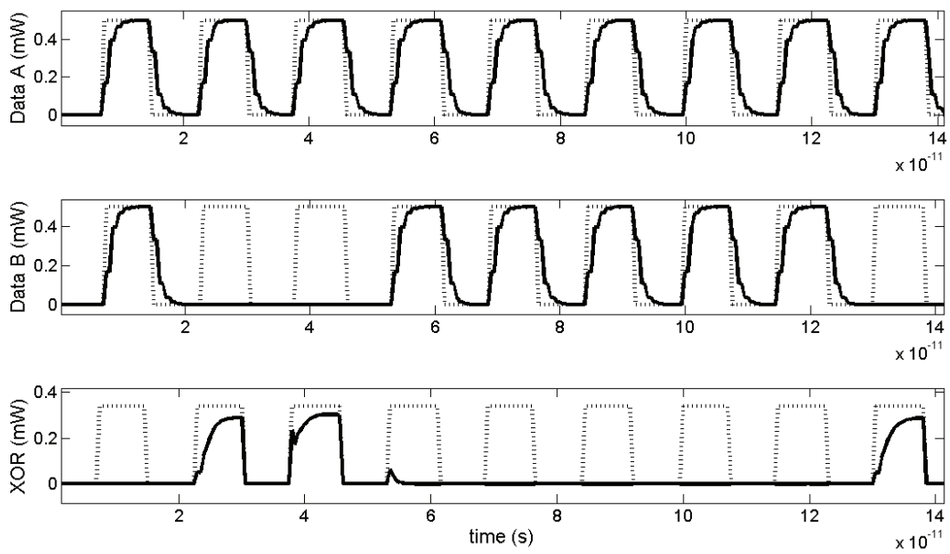

Fig. 9. XOR operation with a clock stream at a signal bit rate $100Gb/s$

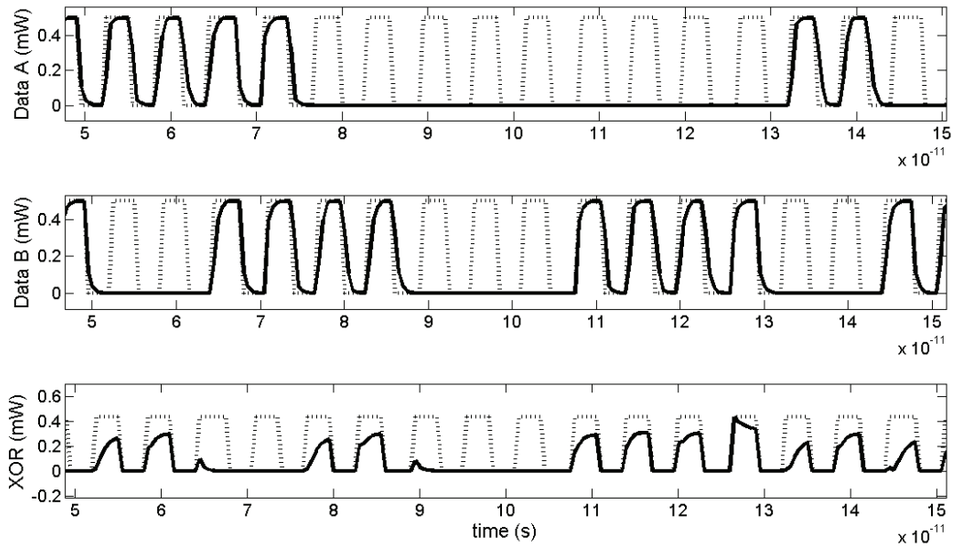

Fig. 10. XOR operation with a clock stream at a signal bit rate $250Gb/s$

medium, and the MZI equations. We have taken into account the two energy levels, namely, ES and GS in the QD conduction band and the inhomogeneity of the QDs size and the resulting inhomogeneous spectral broadening. For a high performance of the proposed processor, LEF should be $\alpha \gtrsim 1$. The QD SOA-MZI based all-optical processor operation rate is limited by the WL-ES electron transition relaxation time and sharply deteriorates with the increase

of repetition rates. The limiting bit rate also depends on the bias current value. Analysis shows that for $I = 30mA$ and $I = 50mA$ the highest bit rates corresponding to the processor successful performance are $100Gb/s$ and $200Gb/s$, respectively.

7. References

Agrawal, G.P. & Olsson, N.A. (1989). Self-phase modulation and spectral broadening of optical pulses in semiconductor laser amplifiers. *IEEE Journal of Quantum Electronics*, Vol. 25, No.11, (November 1989) 2297-2306, ISSN 0018-9197

Agrawal, G.P. (2001). *Applications of Nonlinear Fiber Optics.* Academic Press, ISBN 0-12-045144-1, New York

Agrawal, G.P. (2002). *Fiber-Optic Communication Systems*. Wiley, ISBN 0-471-21571-6, New York

Bányai, L. & Koch, S. W. (2005). *Semiconductor Quantum Dots* (Second Edition). World Scientific, ISBN 9810213905, London,

Ben-Ezra, Y.; Haridim, M. & Lembrikov, B. I. (2005). Theoretical analysis of gain-recovery time and chirp in QD-SOA. *IEEE Photonics Technology Letters*, Vol. 17, No. 9, (September 2005) 1803-1805, ISSN 1041-1135

Ben-Ezra, Y.; Lembrikov, B. I. & Haridim, M. (2005). Acceleration of gain recovery and dynamics of electrons in QD-SOA. *IEEE Journal of Quantum Electronics*, Vol. 41, No. 10, (October 2005) 1268-1273, ISSN 0018-9197

Ben-Ezra, Y.; Lembrikov, B. I. & Haridim, M. (2007). Specific features of XGM in QD-SOA. *IEEE Journal of Quantum Electronics*, Vol.43, No. 8, (August 2007) 730-737, ISSN 0018-9197

Ben-Ezra, Y.; Haridim, M.; Lembrikov, B.I. & Ran, M. (2008). Proposal for All-optical Generation of Ultra Wideband Impulse Radio Signals in Mach-Zehnder Interferometer with Quantum Dot Optical Amplifier. *IEEE Photonics Technology Letters*, Vol. 20, No. 7 (April 2008) 484-486, ISSN 1041-1135

Ben-Ezra, Y.; Lembrikov, B.I. & Haridim, M. (2009). Ultra-Fast All-Optical Processor Based on Quantum Dot Semiconductor Optical Amplifiers (QD-SOA). *IEEE Journal of Quantum Electronics*, Vol. 45, No.1 (January 2009) 34-41, ISSN 0018-9197

Berg, T.W.; Bischoff, S.; Magnusdottir, I. & Mørk, J. (2001). Ultrafast gain recovery and modulation limitations in self-assembled quantum-dot devices. *IEEE Photonics Technology Letters*, Vol. 13, No. 6 (June 2001) 541-543, ISSN 1041-1135

Berg, T.W.; Mørk, J. & Hvam, J.M. (2004). Gain dynamics and saturation in semiconductor quantum dot amplifiers. *New Journal of Physics*, Vol. 6, No. 178, (2004) 1-23, ISSN 1367-2630

Berg, T.W. & Mørk, J. (2004). Saturation and Noise Properties of Quantum-Dot Optical Amplifiers. *IEEE J. of Quantum Electronics*, Vol. 40, No. 11, (November 2004) 1527-1539, ISSN 0018-9197

Bimberg, D.; Grundmann, M. & Ledentsov, N. N. (1999). *Quantum Dot Heterostructures*. John Wiley, ISBN 047 1973882, New York

Chen, H.; Zhu, G.; Wang, Q.; Jaques, J.; Leuthold, J.; Picirilli, A.B. & Dutta, N.K. (2002). All-optical logic XOR using differential scheme and Mach-Zender interferometer. *Electronic Letters*, Vol. 38, No. 21, (October 2002) 1271-1273, ISSN 0013-5194

Dagens, B.; Markus, A.; Chen, J.X.; Provost, J.-G.; Make, D.; de Gouezigou, O.; Landreau, J.; Fiore, A. & Thedrez, B. (2005). Giant linewidth enhancement factor and purely frequency modulated emission from quantum dot laser, *Electronics Letters*, Vol. 41, No. 6, (17th March 2005) 323-324, ISSN 0013-5194

Dong, J.; Zhang, X.; Fu, S.; Xu, J.; Shum, P. & Huang, D. (2008) Ultrafast all-optical signal processing based on single semiconductor optical amplifier. *IEEE Journal of Selected Topics in Quantum Electronics*, Vol. 14, No. 3 (May/June 2008) 770-778, ISSN 1077-260X

Gehrig, E. & O. Hess, O. (2002). Mesoscopic spatiotemporal theory for quantum-dot lasers. *Phys. Rev. A,* Vol. 65, No. 3, (March 2002) 033804-1-16, ISSN 1050-2947

Hamié, A.; Sharaiha, A.; Guégan, M. & Pucel, B. (2002). All-Optical logic NOR Gate Using Two-Cascaded Semiconductor Optical Amplifiers. *IEEE Photonics Technology Letters*, Vol. 14, No. 10, (October 2002) 1439-1441, ISSN 1041-1135

Joergensen, C. ; Danielsen, S.L.; Durhuus, T.; Mikkelsen, B. ; Stubkjaer, K.E.; Vodjdani, N.; Ratovelomanana, F.; Enard, A.; Glastre, G.; Rondi, D. & Blondeau, R. (1996). Wavelength conversion by optimized monolithic integrated Mach-Zender interferometer, *IEEE Photonics Technology Letters,* Vol. 8, No. 4, (April 1996) 521-523, ISSN 1041-1135

Kanellos, G.T.; Petrantonakis, D.; Tsiokos, D.; Bakopoulos, P.; Zakynthinos, P.; Pleros, N.; Apostolopoulos, D.; Maxwell, G.; Poustie, A. & Avramopoulos, H. (2007). All-optical 3R burst-mode reception at 40 Gb/s using four integrated MZI switches. *Journal of Lightwave Technology*, Vol. 25, No. 1, (January 2007) 184-192, ISSN 0733-8724

Kim, J.; Laemmlin, M.; Meuer, C.; Bimberg, D. & Eisenstein, G. (2009). Theoretical and experimental study of high-speed small-signal cross-gain modulation of quantum-dot semiconductor optical amplifiers. *IEEE J. of Quantum Electronics*, Vol. 45, No. 3, (March 2009) 240-248, ISSN 0018-9197

Leem, Y.A.; Kim, D. C.; Sim, E.; Kim, S.-B.; Ko, H.; Park, K.H.; Yee, D.-S.; Oh, J. O.; Lee, S. H. & Jeon, M. Y. (2006). The characterization of all-optical 3R regeneration based on InP-related semiconductor optical devices, *IEEE J. of selected topics in Quantum Electronics*, Vol. 12, No. 4, (July/August 2006) 726-735, ISSN 1077-260X

Matthews, D.K. ; Summers, H.D.; Smowton, P.M.; Blood, P.; Rees, P. & Hopkinson, M. (2005). Dynamics of the wetting-layer-quantum-dot interaction in GaAs self-assembled systems, *IEEE Journal of Quantum Electronics*, Vol. 41, No. 3, (March 2005), 344-350, ISSN 0018-9197

Mukherjee, B. & Zang, H. (2001). Introduction. Survey of State-of-the-Art, In: *Optical WDM Networks. Principles and Practice,* Sivalingam, K.M. & Subramaniam, S. (Ed.), 3-24, Kluwer, ISBN 0-7923-7825-3, Boston

Newell, T.C.; Bossert, D.J.; Stinz, A.; Fuchs, A. & Malloy, K.J. (1999). Gain and linewidth enhancement factor in InAs quantum-dot laser diodes, *IEEE Photonics Technology Letters*, Vol. 11, (November 1999), 1527-1529, ISSN 1041-1135

Ohtsu, N.; Kobayashi, K.; Kawazoe, T.; Yatsui, T. & Naruse, N. (2008). *Principles of Nanophotonics,* CRC Press, ISBN-13 978-1-58488-972-4, London

Qasaimeh, O. (2003). Optical gain and saturation characteristics quantum-dot semiconductor optical amplifiers. *IEEE J. of Quantum Electronics*, Vol. 39, No. 6, (June 2003) 793-798, ISSN 0018-9197

Qasaimeh, O. (2004). Characteristics of cross-gain (XG) wavelength conversion in quantum dot semiconductor optical amplifiers. *IEEE Photonics Technology Letters*, Vol. 16, No. 2, (February 2004) 542-544, ISSN 1041-1135

Ramamurthy, B. (2001). Swithches, wavelength routers, and wavelength converters. In: *Optical WDM Networks. Principles and Practice,* Sivalingam, K.M. & Subramaniam, S. (Ed.), 51-75, Kluwer, ISBN 0-7923-7825-3, Boston

Sakamoto, A. & Sugawara, M. (2000). Theoretical calculation of lasing spectra of quantum-dot lasers: effect of homogeneous broadening of optical gain, *IEEE Photonics Technology Letters*, Vol. 12, No. 2, (February 2000) 107-109, ISSN 1041-1135

Sartorius, B. (2001). 3R regeneration for all-optical networks, *Proceedings of 3rd International Conference on Transparent Optical Networks* (ICTON 2001), Th. A.4, pp. 333-337, ISBN 10 0780370961, Krakow, Poland, June 18-21, IEEE, Krakow

Schneider, S.; Borri, P.; Langbein, W.; Woggon, U.; Sellin, R.L.; Ouyang, D. & Bimberg, D. (2004). Linewidth enhancement factor in InGaAs quantum-dot amplifiers, *IEEE of Quantum Electronics*, Vol. 40, No. 10, (October 2004) 1423-1429, ISSN 0018-9197

Sugawara, M.; T. Akiyama, T.; N. Hatori, N. ; Y. Nakata, Y.; Ebe, H. & H. Ishikava, H. (2002). Quantum-dot semiconductor optical amplifiers for high-bit-rate signal processing up to 160 Gbs^{-1} and a new scheme of 3R regenerators, *Measurement Science and Technology*, Vol. 13, (2002), 1683-1691, ISSN 0957-0233

Sugawara, M.; Ebe, H.; Hatori, N.; Ishida, M.; Arakawa, Y.; Akiyama, T.; Otsubo, K. & Nakata, Y. (2004) Theory of optical signal amplification and processing by quantum-dot semiconductor optical amplifiers. *Phys. Rev.B,* Vol. 69, No. 23 (June 2004) 235332-1-39, ISSN 1098-0121

Sun, G.; Khurgin, J.B. & Soref, R.A. (2004). Design of quantum-dot lasers with an indirect bandgap short-period superlattice for reducing the linewidth enhancement factor, *IEEE Photonics Technology Letters,* Vol.16, No. 10 (October 2004), 2203-2205, ISSN 1041-1135

Sun, H.; Wang, Q.; Dong, H. & Dutta, N.K. (2005). XOR performance of a quantum dot semiconductor optical amplifier based Mach-Zender interferometer, *Optics Express*, Vol. 13, No. 6, (March 2005) pp.1892-1899, ISSN 10944087

Uskov, A.V. ; Berg, T.W. & Mørk, J. (2004). Theory of pulse-train amplification without patterning effects in quantum-dot semiconductor optical amplifiers. *IEEE J. of Quantum Electronics*, Vol. 40, No. 3, (March 2004) 306-320, ISSN 0018-9197

Ustinov, V.M.; Zhukov, A.E.; Egorov, A. Yu. & Maleev, N. A. (2003). *Quantum Dot Lasers,* Oxford University Press, ISBN 0 19 852679 2, Oxford

Wada, O. (2007). Femtosecond all-optical devices for ultrafast communication and signal processing, In: *Microwave Photonics,* Lee, C. H. (Ed), 31-75, CRC Press, ISBN-10: 0-8493-3924-3

Wang, Q.; Zhu, G.; Chen, H. ; Jaques, J. ; Leuthold, J.; Picirilli, A.B. & Dutta, N.K. (2004). Study of all-optical XOR using Mach-Zehnder interferometer and differential scheme. *IEEE J. of Quant. Electr.*, Vol. 40, No. 6, (June 2004) 703-710, ISSN 0018-9197

Zhu, Z.; Funabashi, M.; Zhong Pan; Paraschis, L.; Harris, D. & Ben Yoo, S.J. (2007). High-performance optical 3R regeneration for scalable fiber transmission system applications", *Journal of Lightwave Technology*, Vol. 25, No. 2, (January 2007) 504-511, ISSN 0733-8724

Semiconductor Technologies

Edited by Jan Grym

ISBN 978-953-307-080-3
Hard cover, 462 pages
Publisher InTech
Published online 01, April, 2010
Published in print edition April, 2010

Semiconductor technologies continue to evolve and amaze us. New materials, new structures, new manufacturing tools, and new advancements in modelling and simulation form a breeding ground for novel high performance electronic and photonic devices. This book covers all aspects of semiconductor technology concerning materials, technological processes, and devices, including their modelling, design, integration, and manufacturing.

How to reference

In order to correctly reference this scholarly work, feel free to copy and paste the following:

Y. Ben Ezra and B.I. Lembrikov (2010). New Approach to Ultra-Fast All-Optical Signal Processing Based on Quantum Dot Devices, Semiconductor Technologies, Jan Grym (Ed.), ISBN: 978-953-307-080-3, InTech, Available from: http://www.intechopen.com/books/semiconductor-technologies/new-approach-to-ultra-fast-all-optical-signal-processing-based-on-quantum-dot-devices

INTECH
open science | open minds

InTech Europe
University Campus STeP Ri
Slavka Krautzeka 83/A
51000 Rijeka, Croatia
Phone: +385 (51) 770 447
Fax: +385 (51) 686 166
www.intechopen.com

InTech China
Unit 405, Office Block, Hotel Equatorial Shanghai
No.65, Yan An Road (West), Shanghai, 200040, China
中国上海市延安西路65号上海国际贵都大饭店办公楼405单元
Phone: +86-21-62489820
Fax: +86-21-62489821

IntechOpen